Self-Assembly of Protein Fibrils into Supra-Fibrillar Aggregates: Bridging the Nano- and Mesoscale

*Slav A. Semerdzhiev[†], Dirk R. Dekker[†], Vinod Subramaniam[†‡§], and Mireille M.A.E. Claessens[†‡] ***

[†] Nanobiophysics, MESA+ Institute for Nanotechnology, Faculty of Science and Technology University of Twente, PO Box 217, 7500 AE Enschede, The Netherlands,

[‡] MIRA Institute for Biomedical Technology and Technical Medicine, University of Twente, PO Box 217, 7500 AE Enschede, The Netherlands

[§] FOM Institute AMOLF, Science Park 104, 1098 XG Amsterdam, The Netherlands

Address correspondence to: m.m.a.e.claessens@utwente.nl

We report on *in vitro* self-assembly of nanometer sized α-synuclein amyloid fibrils into well-defined micrometer sized supra-fibrillar aggregates with sheet-like or cylindrical morphology depending on the ionic strength of the solution. The cylindrical supra-fibrillar structures are heavily hydrated, suggesting swollen gel-like particles. In contrast to higher order structures

formed by other negatively charged biopolymers, multivalent ions are not required for the supra-fibrillar aggregates to form. Their formation is induced by both mono- and divalent counterions. The self-assembly process is not mediated by protein specific interactions but rather by the cooperative action of long-range electrostatic repulsion and short-range attraction. Understanding the mechanism driving the self-assembly might give us valuable insight into the pathological formation of fibrillar superstructures such as Lewy bodies and neurites - distinct signatures of Parkinson's disease - and will open the possibility to utilize the self-assembly process for the design of novel fibril-based smart nanostructured materials.

The self-assembly of proteins into amyloids appears to be a generic phenomenon.[1-2] A common architectural motif of amyloid fibrils is the characteristic cross-β spine comprised of β-strands oriented perpendicularly to the longitudinal fibril axis. The connection of protein monomers *via* multiple hydrogen bonds parallel to the fibril's growth direction results in fibrils with diameters of 1-10 nm and lengths of >100 nm.[3] Due to their architecture, amyloid fibrils are extremely robust against chemical destabilization and mechanical stress. Thus, once formed they remain intact and accumulate.

In tissues fibrils accumulate in supra-fibrillar assemblies with dimensions up to tens of micrometers. Such supra-fibrillar structures are a distinct signature of many neurodegenerative diseases.[4] In the case of Parkinson's disease, fibrillar α-synuclein (αS) is deposited in supra-fibrillar aggregates known as Lewy bodies and neurites.[5] The pathological significance of these structures and formation mechanisms remain to be elucidated. Cell toxicity has been attributed to both prefibrillar αS aggregates (oligomers) and fibrillar αS but there is no general consensus on which species is most potent in disrupting the cell's normal

functioning.[6-7] It has been proposed that the formation of αS fibrillar inclusion bodies is a result of a cellular defense machinery responsible for the interception and sequestration of harmful protein aggregates within the cell through active retrograde transport.[8] However, there is evidence that under certain conditions fibrils of some amyloidogenic proteins and peptides spontaneously assemble into higher order structures suggesting that a more generic physicochemical process could also be involved in the formation of intracellular fibril assemblies.[9-12]

Amyloid formation and higher order organization is not necessarily associated with a disease condition. Nature has utilized the advantageous features of amyloids to devise functional materials. For example, amyloid networks are used as a storage system for hormones in glands and other organs and as adhesives by barnacles or *E. coli* to deploy their colonies on different surfaces.[13-15] Some fish and insect species exploit the chemical and mechanical stability of amyloid fibrils – comparable to those of silk and steel – by using them as a reinforcing scaffold protecting their eggs from damage.[16-18] These and many more examples classify amyloids as an attractive candidate for the design of novel bio-inspired materials. However, to profit from the advantageous properties of amyloids and to construct materials that are ordered at both the nano- and micro-scale a better understanding of the interactions driving the multi-scale self-assembly is required.

In many aspects – high charge density, morphological features and rigidity - αS fibrils resemble other filamentous biopolyelectrolytes such as DNA, F-actin and microtubules. The aforementioned biopolymers form higher order structures in the presence of multivalent counterions through various interaction mechanisms.[19-23] The attraction between rods with the same charge can be mediated through correlated movement of condensed counterions on the rods' charged surfaces resembling van der Waals interactions.[24-27] It has even been suggested that the positions of condensed counterions on the rods' surfaces can become so strongly

correlated that they adopt a Wigner crystal-like arrangement. The cohesive energy of this kind of crystal structure then acts as a source of the attractive interaction.[28-31] Experimental observations have indeed revealed counterion density fluctuations coupled to the twisted topography of the polyelectrolyte's charged surface giving rise to "zipper-like' charge alignment.[32]

The self-assembly of αS into nano-sized amyloid fibrils has been studied in the past decades due to its relation with Parkinson's disease. However, the scope of those studies has rarely gone beyond the organization of the protein at the nano-scale.[33] Given the morphological similarity between αS amyloid fibrils and other self-organizing charged rod-like biopolymers we anticipate a higher-order organization of αS fibrils. To understand the self-assembly of fibrils into defined structures and to elucidate the forces driving this phenomenon we investigate the higher order organization of αS fibrils by systematic variation of physico-chemical parameters such as pH, temperature and ionic strength.

RESULTS AND DISCUSSION

Formation of supra-fibrillar aggregates

The formation of αS amyloid fibrils is induced by incubating the protein in buffered solution at 37 $^{\circ}$C under constant agitation. The incubation time necessary to obtain the fibrils varies from hours to several days depending on aggregation conditions used such as pH, ionic strength, temperature, protein concentration and seeding. To follow fibril formation in time, αS aggregation is monitored using the amyloid binding dye Thioflavin T (ThT). The time resolved ThT fluorescence intensity trace attains the typical sigmoidal shape characteristic for the nucleation and growth mechanism accompanying the amyloid fibril formation (SI Figure S1). Under the experimental conditions used in this study (see Materials and Methods section) the sample becomes turbid within 10 hours after the aggregation is initiated indicating the

evolution of large structures in the solution. Visual inspection of the aggregated samples with optical microscopy surprisingly revealed the presence of entirely new species of protein aggregates. The sample is densely populated by protein assemblies with a cylindrical morphology and a fairly narrow size distribution (Figures 1A, 1B and S2). The high ThT fluorescence intensity of the self-assembled structures (Figure 1B) indicates amyloid content. Atomic force (Figures 2C, 2D) and high resolution scanning electron (SI Figure S3) micrographs confirm that the structures are indeed comprised of fibrillar αS. It also can be seen from the images that individual and clustered fibrils are still present in the sample indicating that not all of the fibrillar protein is incorporated in the self-assembled structures. 3D reconstructed confocal laser scanning microscope (CLSM) images of supra-fibrillar aggregates grown with addition of fluorescently labeled αS140C monomers (see Material and Methods) at different time points during the self-assembly process show how the structures evolve in time (Figure 3). The observed layered patterns suggest that growth propagates radially from the central longitudinal axis of the supra-fibrillar aggregates towards the periphery. Once dried on a mica surface the structures collapse to sheets with thickness ~640 nm (Figure 2B) and a general shape the same as that observed for the swollen structures in solution. This observation suggests that these structures are heavily hydrated. Calculations generate a rough estimate for a water content of ≥90 % (SI 1); a significant fraction of the aggregate's volume can be assigned to the solvent. This implies a gel-like architecture of the supra-fibrillar aggregates.

Long-range electrostatic repulsion

The highly charged C-terminal part (Figure 4) of αS and compact structure of the cross β-sheet fibril core yields amyloid fibrils with a high surface charge density. Attractive interactions between like-charged semi-flexible polyelectrolytes have been observed in multiple systems. At sufficiently high concentrations of multivalent counterions

biopolyelectrolytes such DNA, microtubules, F-actin, viruses and viral capsid particles are able to self-organize into higher order structures.[19-23] Similarly, αS supra-fibrillar assemblies require sufficiently high salt concentrations to form. At low ionic strength the solution mainly contains individual αS fibrils as the interfibril repulsion is too strong. With increasing salt concentration electrostatic effects are gradually screened making it possible for the fibrils to come in proximity. As a result, increasing quantities of fibrillar sheet-like structures appear and the fraction of individual fibrils decreases (Figure 5). Further increments in the ionic strength gradually lead to the appearance of cylindrical aggregates coexisting with supra-fibrillar sheets, and at even higher salt concentrations mainly the former species remains visible in the solution. The formation of the higher order fibrillar assemblies seems to be invariant to the chemical nature of the counterions used to induce the self-assembly process. Despite the fact that αS has a divalent metal binding site and a calcium binding motif, [34-36] there are no observable differences in the phase behavior in the presence of Ca^{2+} or Mg^{2+}. Even more surprisingly, and contrary to other biopolyelectrolyte systems, αS fibrils cluster into higher order structures irrespective of the valence of the counterions. Albeit at different concentrations, both the monovalent (NaCl and KCl) and divalent ($CaCl_2$ and $MgCl_2$) salts are equally successful in inducing the formation of higher order assemblies (Figure 5D and 5E). The condensation of fibrils in the presence of monovalent counterions suggests that counterion condensation is not responsible, or at least not the only mechanism giving rise to an attractive interfibril potential driving the self-assembly phenomenon. This assumption is in agreement with theoretical predictions for the interactions of two parallel rod-like polyelectrolytes carrying the same charge. In the presence of monovalent salts the onset of attractive interactions between the rods due to correlated fluctuations of condensed counterions is at very short distances where the rods practically start to sterically hinder one another.[24] However, one cannot discard the option that counterion condensation contributes to

the attractive potential between filaments in the presence of multivalent ions since the interactions in this case are more long-ranged. Given the high charge density at the fibril's surface it is expected that counterion condensation takes place at any salt condition. Therefore, correlated motions of condensed multivalent counterions along the rods most likely play an important role in the aggregation of fibrils into higher order assemblies.

The independence of the fibril to supra-fibrillar aggregate transition on the chemical nature of the counterions and the strong influence of the counterion valence on the transition point suggest that the high salt concentrations are mainly necessary to sufficiently screen electrostatics. This assertion is further confirmed in experiments in which the charge on the fibrils is modulated by pH or use of a αS deletion mutant lacking the charged C-terminal part (Figure 4). Amyloid fibrils of wild type αS do assemble into supra-fibrillar aggregates in absence of salt as long as the pH is set close to the isoelectric point of the protein of 4.7. Increasing the pH to higher values leads to recovery of the negative charges and eventually the repulsion becomes too strong, forcing the preformed aggregates to disassemble into individual αS amyloid fibrils (Figure 6). The αS 1-108 truncation mutant (Figure 4) is slightly positively charged at neutral pH and still able to form amyloid fibrils.[37] Interestingly the αS 1-108 fibrils retain their ability to form higher order fibrillar assemblies throughout the whole salt concentration range used and even in the absence of added salt (Figure 1C). These findings further confirm that the formation of wild type αS supra-fibrillar aggregates at low ionic strength is mainly prevented by the excessive interfibrillar electrostatic repulsion. Once the charge is sufficiently screened, short-ranged attraction takes over and drives the fibrils into the assembly. However, the persisting ability of αS 1-108 to form supra-fibrillar aggregates has another important implication. In agreement with what was previously postulated, it hints at the presence of attractive interactions originating from a different source than correlated movements of condensed counterions.

Finite size of the supra-fibrillar aggregates

There is another important role in the self-assembly process that can be assigned to the electrostatic interactions. Electrostatic interactions seem to dictate the development of supra-fibrillar aggregates into finite sized objects. The experimental findings suggest that the growth of the aggregates is not simply limited by depletion of monomers and fibrils from solution. Increasing the ionic strength of a solution of supra-fibrillar aggregates and subsequent addition of pregrown fibrils results in formation of additional layers in the supra-fibrillar structures (Figure 7C). On the other hand, reduction of the ionic strength deteriorates the charge screening and the added fibrils do not condense on the aggregate's surface to form supplementary layers (Figure 7B). These findings allow us to reason that the growth of the aggregates is probably contained by the electrostatic energy buildup that cannot be compensated for with newly-established interfibrillar contacts. Such an interplay between long-range repulsion and short-range attraction is not uncommon and has been shown to stabilize aggregating colloidal systems giving rise to the formation of finite-sized aggregates.[38-40] Considering the long-range character of electrostatic interactions, the accumulation of charge can indeed result in buildup of excessive electric potential at the surface of the growing aggregates, preventing further addition of αS fibrils. Given the size of the aggregates (d = 10 - 20 μm) and assuming a homogeneous distribution of material throughout the aggregate's volume, the latter hypothesis looks unlikely but remains plausible. Another possible explanation of the observed phenomenon is the depletion of "free" counterions from the bulk. Due to their high surface charge densities, αS fibrils most probably concentrate (or even condense) a significant amount of counterions in their ionic atmosphere to sufficiently screen the electrostatic repulsion and consequently to cluster. The latter scenario can also be considered from a slightly different perspective where the growth of the supra-fibrillar aggregates is not limited because of counterion depletion but rather because of

the significant loss of counterion entropy. It is possible that at some point further cohesive contacts between fibrils cannot energetically compensate the entropy loss originating from the confinement of counterions in the vicinity of the fibril's surface.

Short-ranged attraction: Hydrophobic interactions

The ability of αS 1-108 fibrils to assemble into supra-fibrillar aggregates in the absence of salt and the formation of full length αS supra-fibrillar structures in the presence of only monovalent salt implies the presence of another source of inter-fibril attraction than counterion condensation. The profound effect that temperature has on the fibril clustering suggests that the short-range attraction is most probably of entropic origin. Higher temperatures shift the transition point from fibrils to higher order structures towards lower salt concentrations. Aggregating 100 μM wild type αS solution with 10 mM $CaCl_2$ at 37°C results in the formation of a mixture of fibrils and very low number of small aggregates (Figure 8A). Incubating this solution at 60 ^{o}C enhances fibril clustering leading to a reduction in the free fibrils fraction and formation of bigger fibrillar aggregates (Figure 8B and 8D). Incubating the fibrillar solution (formed at 10 mM $CaCl_2$ at 37°C) at 80 ^{o}C reinforces the effect observed in the 60 ^{o}C sample, and as a result all the available fibrils cluster (Figure 8D) to form even bigger aggregates (Figure 8C). The influence of temperature on the clustering of fibrils does not stem from possible temperature induced differences in fibril morphology. The enhancing effect of temperature on the fibril clustering is probably due to the presence of hydrophobic domains in the fibrils that are exposed to unfavorable contacts with the solvent. Such hydrophobic solvation is entropically penalized and thus higher temperature fosters a process that ultimately leads to shielding of the hydrophobic patches on the fibril surface from the surrounding polar medium. The presence of hydrophobic domains on αS fibrils would not be a surprise given the amino acid sequence of the protein and the architecture of the fibrils. The amino acid composition of the central region (NAC region) of the protein sequence is

dominated by hydrophobic residues and is believed to be responsible for αS aggregation and fibril formation.[41] Even though there is no general consensus on the subtle details regarding the exact architecture of the αS fibril, the general structural blueprint that emerges from all the studies concerns a fibril with hydrophobic core including the NAC region and solvent exposed C-terminal part.[42] It is possible that yet some surface from the hydrophobic core in the mature fibril remains solvent exposed or is being exposed upon compaction of the C-terminal segment when the charges are abolished at low pH or screened with salt.[43] Nevertheless, the strong promoting effect of temperature on fibril aggregation remains surprising. Besides reinforcing hydrophobic interactions, elevated temperatures influence charge screening. Considering the dependence of the Debye length on the temperature – the size of the double electric layer scales with $T^{1/2}$ - increasing the temperature should deteriorate charge screening, *i.e.* stabilize the fibrils against clustering. However, the hydrophobic effect seems to be the dominant one in the balance resulting in net increase of the interfibrillar attraction.

CONCLUSION

In summary we have shown that αS hierarchically self-assembles into finite sized supra-fibrillar aggregates with well-defined morphology spanning the gap between nano- and microscale. The self-assembly process is a consequence of the interplay between long-ranged repulsive and short-ranged attractive interactions. The repulsive part of the interactions stems from the high net negative charge on the αS fibrils. Additionally, the charge on the fibrils has a regulatory role in the growth process of the aggregates. Rather than only resulting from the correlated movement of condensed counterions, the attractive part of the interactions seems to be of entropic origin. Attraction resulting from counterion correlation cannot be excluded when multivalent ions are present in the aggregating solution. Finally it is important to point

out that the observed self-assembly process is not only interesting from a materials science perspective. The interactions governing the fibril clustering may also have physiological implications. The *in vitro* generated supra-fibrillar aggregates – no matter what morphology – start appearing at physiologically relevant protein concentrations and ionic strength. Within the brain αS represents 0.5-1% of the total protein content equating to approximately 20-40 μM.[44] The magnesium levels within the cell are in the 800 μM range, while the sodium and potassium levels are around 14 mM and 140 mM respectively. The total ionic strength in the cytosol is most likely in the range where the fibrils have an enhanced propensity to self-aggregate. Thus, once fibrils are formed *in vivo* they may be predisposed to cluster and generate supra-fibrillar assemblies such as Lewy bodies and neurites.

MATERIALS AND METHODS

Preparation and labeling of αS monomers

Expression of the human αS wild type (αSWT), the140C mutant (αS140C) with a single alanine to cysteine substitution at residue 140 and the truncated 1-108 (αS 1-108) mutant missing the last 32 amino acid residues from its original sequence were performed in E. coli B121 (DE3) using the pT7-7 based expression system. Details on the purification procedure for αSWT and αS140C are described elsewhere.[45] The αS 1-108 was purified using the Resource S column (GE Healthcare Lifesciences, UK). The start buffer used was 50 mM glycine at pH 3.3. For the elution step the glycine buffer was supplemented with 1M NaCl. Purified protein was concentrated using Centrisart C4 centrifugal microconcentrators (Sigma-Aldrich, USA) with a 5kD cut-off prior to desalting. The desalting step was carried out using PD-10 columns (GE Healthcare Lifesciences, UK). αSWT and αS-A140C were conjugated with AlexaFluor 405 succinimidyl ester or AlexaFluor 647 maleimide (Life Technologies, USA) following the manufacturer's labeling protocols for both fluorescent probes.

Cylindrical supra-fibrillar aggregates

If not mentioned otherwise, aggregations were sped up by shaking the solutions at 900 rpm. The cylindrical supra-fibrillar aggregates where grown in 10 mM TRIS buffer, pH = 7.4, 37 ^{o}C, 100 µM total protein concentration, and 2 mM CaCl$_2$. For the αS 1-108 mutant no salt was added in the aggregation buffer. To study the effect of salt concentration on the formation of aggregates, the 10mM Tris buffer, pH=7.4, was supplemented with different concentrations of NaCl, KCl, CaCl$_2$ or MgCl$_2$. To assess the aggregation state of the fibrils at different salt conditions phase contrast images were taken using a TE2000 microscope (Nikon, Japan) in transmission mode using a PlanFluor 60x Ph1 DLL objective (Nikon, Japan). To get insight into the time required for completion of aggregation, αSWT aggregates were grown in the presence of 5 µM Thioflavin T (Fluka, Sigma-Aldrich, UK). The Thioflavin T fluorescence intensity at 485 nm was followed in time using Infinite 200 PRO multimode plate reader (Tecan Ltd., Switzerland). For the dual colored aggregates, aggregation was initiated using a mixture of 5000:1 of unlabeled αSWT:αSWT labeled with AlexaFluor 405 succinimidyl ester (αS-Al405). The mixture was then divided in aliquots and incubated at 37° and 900 rpm shaking. Monomers of αS 140C conjugated with AlexaFluor 647 maleimide (αS140C-Al647) were added at different time points to the different aliquots keeping the ratio αSWT: αS140C-Al647 at 5000 : 1. The total (labeled and plain αSWT) protein concentration in the aliquots was 100 µM. When stationary state of the self-assembly process was reached the aliquots were imaged with using a Nikon Eclipse Ti microscope in confocal laser scanning mode. The AlexaFluor 405 and AlexaFluor 647 were excited using 402 nm (CUBE, Coherent Inc., USA) and 647 nm (2RU-VFL-P-300-647, MPB communications Inc., Canada) lasers respectively. The signal from the blue dye was collected using a 450/50 nm bandpass emission filter and from the red one using a 700/75 nm bandpass filter. To study the effect of electrostatic interaction on the growth of the supra-fibrillar structures aliquots of pregrown blue aggregates

(αSWT:αS-Al405 = 5000:1) were incubated with preformed red fibrils (αSWT:αS140C-Al647 = 5000:1) grown at 10 mM TRIS, pH=7.4, 0.1 mM CaCl$_2$, and shaking with 900 rpm 37 ^{o}C. For the low salt conditions prior to the incubation with red fibrils, the pregrown blue aggregates were left at rest for 30 min to sediment and then the supernatant was withdrawn from the sample. The aggregates were resuspended in 10 mM TRIS buffer. The procedure was repeated 3 times to remove the excess salt from the solution. For the higher salt conditions the concentration of CaCl$_2$ in the blue aggregate solution was set to 3 mM prior incubation with the preformed fibrils.

Disk-like aggregates

Aggregates with circular morphology were formed in 2 mM Citric acid, pH = 4.3, shaking with 900 rpm at 37 ^{o}C. Phase contrast images were taken using TE2000 microscope (Nikon, Japan) in transmission mode using a PlanFluor 20x Ph1 DLL objective (Nikon, Japan).

Temperature induced fibril clustering

100 μM αSWT was aggregated in 10 mM TRIS buffer, pH = 7.4, 5 μM Thioflavin T (ThT) 37 ^{o}C, shaking at 900 rpm and 10 mM NaCl for 5 days. Then aliquots of the solution were incubated at 60 ^{o}C and 80 ^{o}C for 3 days. Samples were imaged with a Nikon Ti Eclipse microscope in widefield fluorescence mode. ThT was excited using a mercury lamp (C-HGFIE Intensilight, Nikon) as a light source and the fluorescence signal was collected using 470/70 nm bandpass excitation filter, 495 nm dichroic beam splitter and 525/50 nm bandpass emission filter (49002 - ET – EGFP, Chroma, USA).

Atomic force microscopy

A solution of the supra-fibrillar aggregates was deposited on a mica surface and left at rest for 20 min for the aggregates to sediment and adhere to the substrate. The sample was then gently washed with deionized water (MilliQ, Milipore Corp., USA) and dried with a nitrogen

flow. Height and phase images were obtained using a Multimode 8 AFM (Bruker, USA) in tapping mode using a MSCT Si_3N_4 tip (Bruker AFM probes, USA).
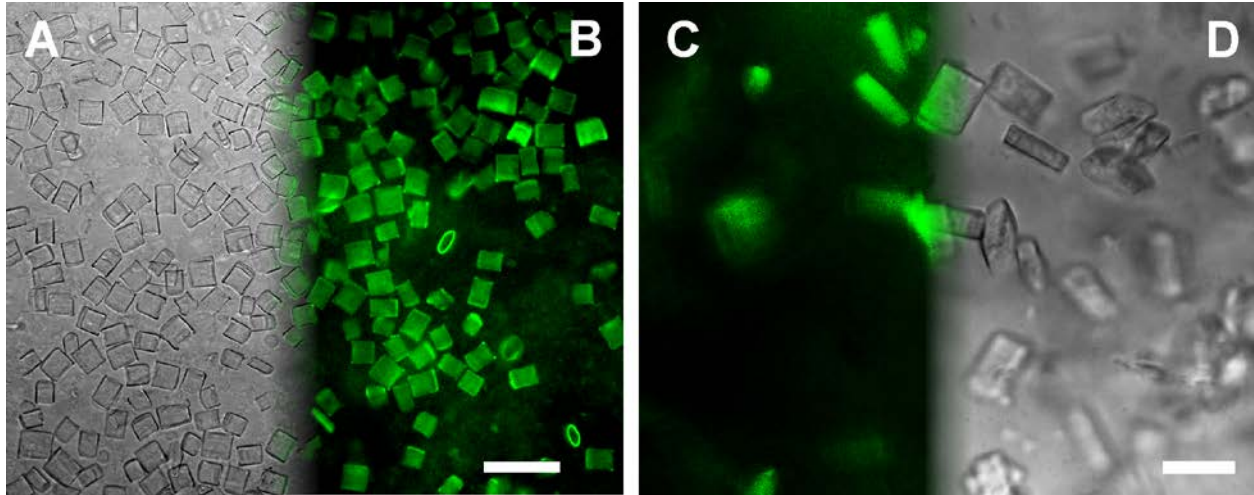
FIGURES

Figure 1. Supra-fibrillar α-synuclein (αS) aggregates. A) Phase contrast and B) fluorescence images of wild type αS cylindrical aggregates formed at 100 μM protein concentration, 2 mM CaCl$_2$, 10 mM Tris buffer, pH = 7.4, 37 ^{o}C and in the presence of 5 μM Thioflavin T. C) Fluorescence and D) phase contrast images of 1-108 truncated αS mutant formed at identical conditions but in a salt free solution (no CaCl$_2$ added). Scale bars are 100 μm (A,B) and 20 μm (C,D).
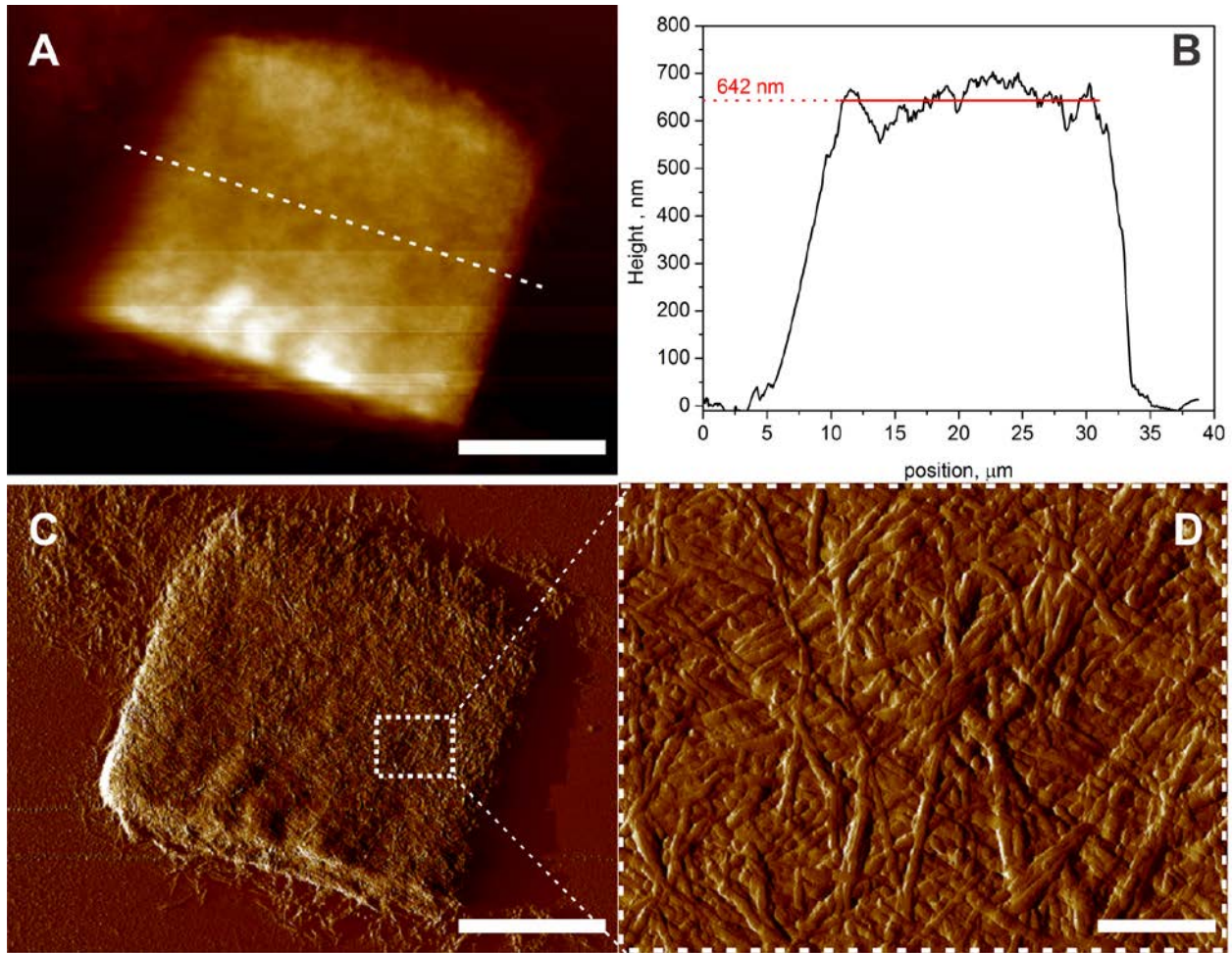
Figure 2. Mesoscopic α-synuclein aggregates are fibrillar. A) Tapping mode AFM micrograph of a dried large αS aggregate collapsed on mica. The overall shape of the tube agrees with the shapes observed in solution. The scale bar is 10μm. B) Cross sectional height profile of the aggregate taken along the dashed line shown in A. The dried aggregates are ≈ 640 nm high. C) Amplitude image of the surface of the aggregate and D) x8 magnification of part of the aggregate's surface. The large aggregates consist of fibrils. Scale bars are 10 μm and 1 μm respectively.
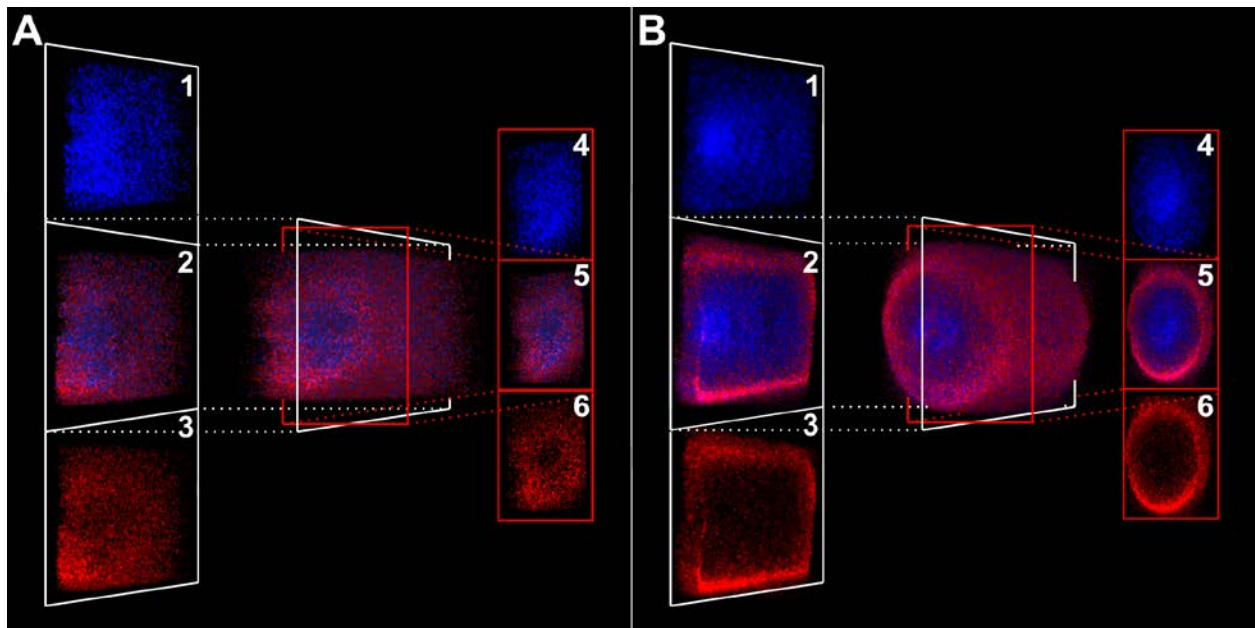
Figure 3. Pattern layers revealing the growth propagation direction of the supra-fibrillar aggregates. Addition of labeled αS monomers different in color than those used to initiate the aggregation, at different time points of the self -assembly process, allows following how the structures evolve in time. A) The 3d image reconstruction (central panel), the longitudinal (1,2,3) and transverse (4,5,6) cross-sections of supra-fibrillar aggregates formed in aliquots to which the αS140C-Al647 monomers were added 15 hours after the aggregation was initiated. B) Identical aliquot to which the monomers were added 25 hours after the aggregation was started.
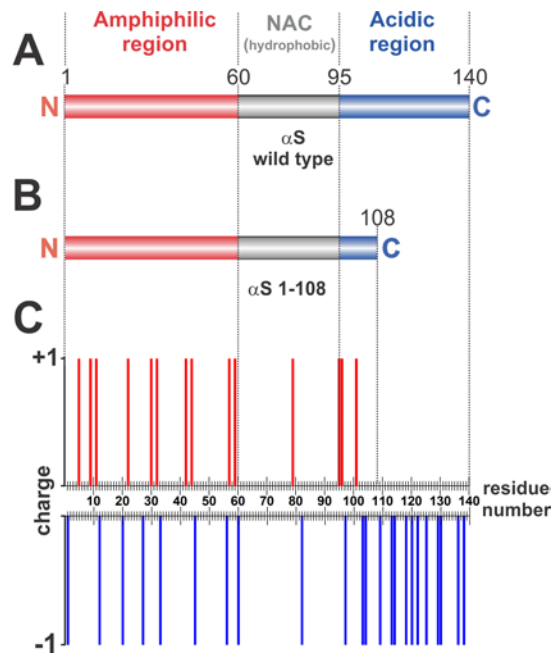
Figure 4. The α-synuclein (αS) molecule. A) The main domain regions in the sequence of wild type (WT) αS. At pH=7.4 αSWT has a net charge ~ -9 and ~ -12 localized on the C-terminal (acidic region). B) αS 1-108 truncated mutant missing the last 32 amino acids residues from the original WT sequence. As a consequence the net charge on the molecule at physiological pH is ~ +3 and ~0 on the remaining C-terminal part. C) Distribution of charged amino acid residues along the sequence of the protein.
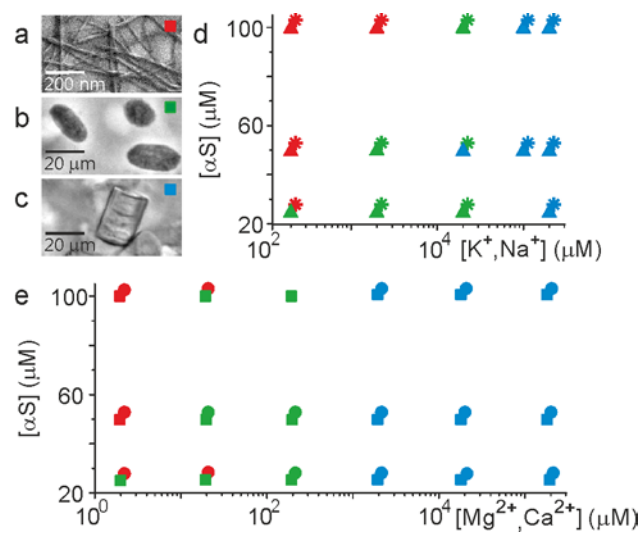
Figure 5. Supra-fibrillar organization of α-synuclein as a function of salt concentration. A) Scanning electron micrograph of fibrils in solution. B-C) Light microscopy images of fibrils organized into fibrillar sheets or condensed into tube shaped supra-fibrillar structures. D) Appearance of the different fibrillar phases as a function of αS, NaCl(▲) and KCl (✱) concentration. E) Organization of fibrils as a function of the CaCl$_2$ (■) and MgCl$_2$ (●) concentrations. The colors in D-E) refer to the structures shown in A-C). At low ionic strength fibrils remain in solution (red) while at high ionic strength most fibrils are present in tube like aggregates. The intermediate regime (green) is characterized by the presence of sheet like structures (B) but tubes (C) are also present. The data shown for aggregation in CaCl$_2$ and MgCl2 represent an average of 3 different protein aggregation experiments.
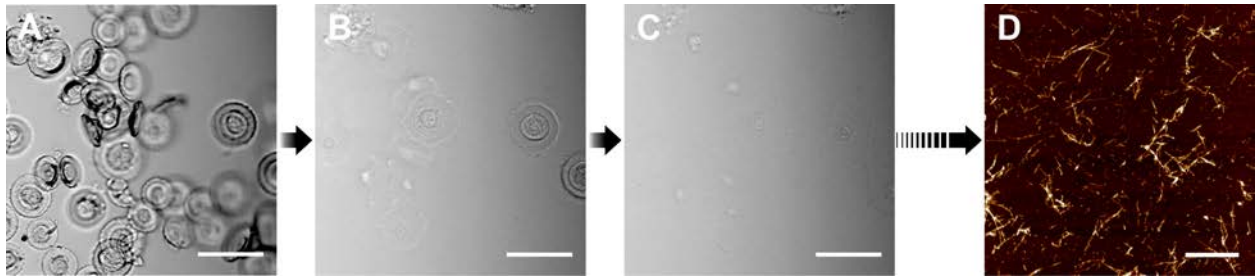
Figure 6. Disassembly of supra-fibrillar αS aggregates. A) Phase contrast image of disk shaped fibrillar aggregates formed at 100 μM αS, 2 mM citric acid, pH 4.3. B,C) Increasing the pH by the addition of NH_3 up to 70 mM charges the protein. The negative charge on the fibrils becomes overwhelmingly high and the aggregates fall apart to fibrils. D) AFM images of the sample from C dried on a mica sheet. Scale bars are 100 μm for A, B, and C and 20 μm for D.
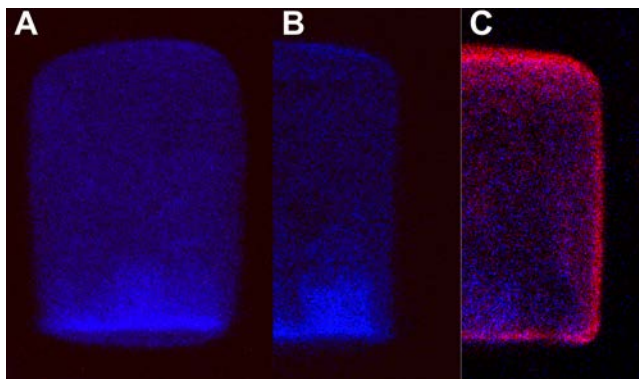
Figure 7. Limited growth of supra-fibrillar aggregates. A) Supra-fibrillar aggregates were initially grown with αS labeled with AlexaFluor 405 in 10 mM Tris, 2 mM $CaCl_2$ until the steady state of the self-assembly procces has been reached. B) Decreasing the salt concentration by washing the blue-labeled fibrillar aggregates with 10 mM Tris buffer and incubating the sample with pre-grown red-labeled fibrils does not induce the formation of additional layers, probably due to charge builldup. C) Increasing the salt concentration up to 3 mM $CaCl_2$ and incubating fraction of the sample with pre-grown fibrils of αS140C mutant labeled with Alexa Fluor 647 leads to buildup of additional layers in the supra-fibrillar structures.
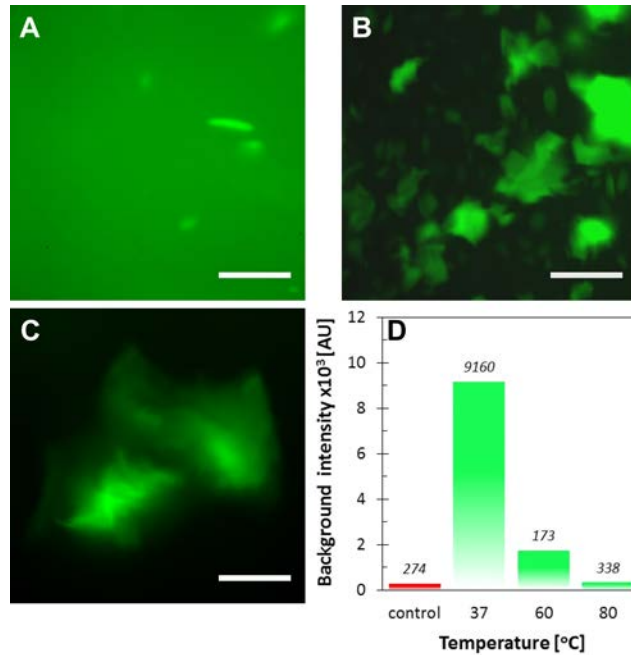
Figure 8. Effect of temperature on filament condensation. The protein fibrils are stained using the β-sheet specific dye Thioflavin T (ThT). A) At 37 °C, 100 μM αS in a 10 mM NaCl and 10 mM Tris buffer at pH 7.4 aggregates into fibrils. The high ThT background fluorescence and the low number of small aggregates indicate that the predominant fraction of fibrils remains free in the solution. B) Part of the αS solution shown in A is incubated at 60 °C. The amount of free fibrils in the solution is reduced and fibrils cluster and big supra-fibrillar structures emerge. C) When the solution from A is incubated at 80 °C all the fibrils condense into even bigger supra-fibrillar structures and none remain free in the solution resulting in a background fluorescence as low as that for the control sample. D) Average values of ThT background fluorescence signal for A, B and C originating from the amyloid fibrils free in the solution. The control sample is identical in composition to those in A, B and C but with only monomeric αS present. Scale bars are 100 μm.

ASSOCIATED CONTENT

Supporting Information Available: **Figure S1.** Time resolved ThT fluorescence intensity curves obtained during formation of αS supra-fibrillar aggregates.; **Figure S2.** Length and width distribution of the SFAs .; **Figure S3.** HRSEM micrographs of a supra-fibrillar aggregate.; **SI 1** Estimation of the water content in the supra-fibrillar aggregates.; **Figure S4.** Geometrical configurations of a swollen and dried supra-fibrillar aggregate used to estimate the water fraction. This material is available free of charge *via* the Internet at http://pubs.acs.org.

AUTHOR INFORMATION

Corresponding Author

M.M.A.E Claessens[†‡*]

University of Twente, PO Box 217, 7500 AE Enschede, the Netherlands

 Tel.:+31 53 489 3157 Fax +31 53 4891105

Email: m.m.a.e.claessens@utwente.nl

Present Addresses

 Nanobiophysics, MESA+ Institute for Nanotechnology, Faculty of Science and Technology, University of Twente, PO box 217, 7500 AE Enschede, The Netherlands

Author Contributions

S.A.S.[†], V.S.[†‡§] and M.M.A.E.C. [†‡*] designed the experiments; S.A.S.[†] and D.R.D.[†] performed the experiments; S.A.S.[†], D.R.D.[†] and M.M.A.E.C.[†‡*] analyzed the data; S.A.S.[†], D.R.D.[†]

V.S.[†‡§] and M.M.A.E.C. [†‡*] wrote the manuscript; All authors have given approval to the final version of the manuscript.

REFERENCES

1. Chiti, F.; Webster, P.; Taddei, N.; Clark, A.; Stefani, M.; Ramponi, G.; Dobson, C. M., Designing Conditions for *in Vitro* Formation of Amyloid Protofilaments and Fibrils. *Proc. Natl. Acad. Sci. U. S. A.* **1999,** *96*, 3590-3594.
2. Chiti, F.; Dobson, C. M., Protein Misfolding, Functional Amyloid, and Human Disease. *Annu. Rev. Biochem.* **2006,** *75*, 333-366.
3. Sunde, M.; Serpell, L. C.; Bartlam, M.; Fraser, P. E.; Pepys, M. B.; Blake, C. C. F., Common Core Structure of Amyloid Fibrils by Synchrotron X-Ray Diffraction. *J. Mol. Biol.* **1997,** *273*, 729-739.

4.   Forman, M. S.; Trojanowski, J. Q.; Lee, V. M. Y., Neurodegenerative Diseases: A Decade of Discoveries Paves the Way for Therapeutic Breakthroughs. *Nat Med* **2004,** *10*, 1055-1063.

5.   Spillantini, M. G.; Schmidt, M. L.; Lee, V. M. Y.; Trojanowski, J. Q.; Jakes, R.; Goedert, M., Alpha-Synuclein in Lewy Bodies. *Nature* **1997,** *388*, 839-840.

6.   Pieri, L.; Madiona, K.; Bousset, L.; Melki, R., Fibrillar Alpha-Synuclein and Huntingtin Exon 1 Assemblies Are Toxic to the Cells. *Biophys. J.* **2012,** *102*, 2894-2905.

7.   Winner, B.; Jappelli, R.; Maji, S. K.; Desplats, P. A.; Boyer, L.; Aigner, S.; Hetzer, C.; Loher, T.; Vilar, M.; Campionic, S.*, et al.*, *In Vivo* Demonstration That Alpha-Synuclein Oligomers Are Toxic. *Proc. Natl. Acad. Sci. U. S. A.* **2011,** *108*, 4194-4199.

8.   Kopito, R. R., Aggresomes, Inclusion Bodies and Protein Aggregation. *Trends in Cell Biology* **2000,** *10*, 524-530.

9.   Donald, A. M., Aggregation in Beta-Lactoglobulin. *Soft Matter* **2008,** *4*, 1147-1150.

10.   Krebs, M. R. H.; MacPhee, C. E.; Miller, A. F.; Dunlop, L. E.; Dobson, C. M.; Donald, A. M., The Formation of Spherulites by Amyloid Fibrils of Bovine Insulin. *Proc. Natl. Acad. Sci. U. S. A.* **2004,** *101*, 14420-14424.

11.   Lara, C.; Adamcik, J.; Jordens, S.; Mezzenga, R., General Self-Assembly Mechanism Converting Hydrolyzed Globular Proteins into Giant Multistranded Amyloid Ribbons. *Biomacromolecules* **2011,** *12*, 1868-1875.

12.   Ridgley, D. M.; Barone, J. R., Evolution of the Amyloid Fiber over Multiple Length Scales. *ACS Nano* **2012**, 1006-1015.

13.   Barlow, D. E.; Dickinson, G. H.; Orihuela, B.; Kulp, J. L.; Rittschof, D.; Wahl, K. J., Characterization of the Adhesive Plaque of the Barnacle Balanus Amphitrite: Amyloid-Like Nanofibrils Are a Major Component. *Langmuir* **2010,** *26*, 6549-6556.

14.   Chapman, M. R.; Robinson, L. S.; Pinkner, J. S.; Roth, R.; Heuser, J.; Hammar, M.; Normark, S.; Hultgren, S. J., Role of Escherichia Coli Curli Operons in Directing Amyloid Fiber Formation. *Science* **2002,** *295*, 851-855.

15.   Maji, S. K.; Perrin, M. H.; Sawaya, M. R.; Jessberger, S.; Vadodaria, K.; Rissman, R. A.; Singru, P. S.; Nilsson, K. P. R.; Simon, R.; Schubert, D.*, et al.*, Functional Amyloids as Natural Storage of Peptide Hormones in Pituitary Secretory Granules. *Science* **2009,** *325*, 328-332.

16.   Iconomidou, V. A.; Vriend, G.; Hamodrakas, S. J., Amyloids Protect the Silkmoth Oocyte and Embryo. *FEBS Lett.* **2000,** *479*, 141-145.

17.   Knowles, T. P.; Fitzpatrick, A. W.; Meehan, S.; Mott, H. R.; Vendruscolo, M.; Dobson, C. M.; Welland, M. E., Role of Intermolecular Forces in Defining Material Properties of Protein Nanofibrils. *Science* **2007,** *318*, 1900-1903.

18.   Podrabsky, J. E.; Carpenter, J. F.; Hand, S. C., Survival of Water Stress in Annual Fish Embryos: Dehydration Avoidance and Egg Envelope Amyloid Fibers. *American Journal of Physiology-Regulatory Integrative and Comparative Physiology* **2001,** *280*, R123-R131.

19.   Haynes, M.; Garrett, R.; Gratzer, W., Structure of Nucleic Acid-Poly Base Complexes. *Biochemistry* **1970,** *9*, 4410-4416.

20.   Needleman, D. J.; Ojeda-Lopez, M. A.; Raviv, U.; Miller, H. P.; Wilson, L.; Safinya, C. R., Higher-Order Assembly of Microtubules by Counterions: From Hexagonal Bundles to Living Necklaces. *Proc. Natl. Acad. Sci. U. S. A.* **2004,** *101*, 16099-16103.

21.   Tang, J. X.; Janmey, P. A., The Polyelectrolyte Nature of F-Actin and the Mechanism of Actin Bundle Formation. *J. Biol. Chem.* **1996,** *271*, 8556-8563.

22.	Tang, J. X.; Wong, S.; Tran, P. T.; Janmey, P. A., Counterion Induced Bundle Formation of Rodlike Polyelectrolytes. *Berichte der Bunsengesellschaft für physikalische Chemie* **1996,** *100*, 796-806.

23.	Wong, G. C. L.; Lin, A.; Tang, J. X.; Li, Y.; Janmey, P. A.; Safinya, C. R., Lamellar Phase of Stacked Two-Dimensional Rafts of Actin Filaments. *Phys. Rev. Lett.* **2003,** *91*.

24.	Oosawa, F., Interaction between Parallel Rodlike Macroions. *Biopolymers* **1968,** *6*, 1633-1647.

25.	Ha, B. Y.; Liu, A. J., Counterion-Mediated Attraction between Two Like-Charged Rods. *Phys. Rev. Lett.* **1997,** *79*, 1289-1292.

26.	Ha, B. Y.; Liu, A. J., Effect of Non-Pairwise-Additive Interactions on Bundles of Rodlike Polyelectrolytes. *Phys. Rev. Lett.* **1998,** *81*, 1011-1014.

27.	Podgornik, R.; Parsegian, V. A., Charge-Fluctuation Forces between Rodlike Polyelectrolytes: Pairwise Summability Reexamined. *Phys. Rev. Lett.* **1998,** *80*, 1560-1563.

28.	GronbechJensen, N.; Mashl, R. J.; Bruinsma, R. F.; Gelbart, W. M., Counterion-Induced Attraction between Rigid Polyelectrolytes. *Phys. Rev. Lett.* **1997,** *78*, 2477-2480.

29.	Kornyshev, A. A.; Leikin, S., Electrostatic Zipper Motif for DNA Aggregation. *Phys. Rev. Lett.* **1999,** *82*, 4138-4141.

30.	Shklovskii, B. I., Wigner Crystal Model of Counterion Induced Bundle Formation of Rodlike Polyelectrolytes. *Phys. Rev. Lett.* **1999,** *82*, 3268-3271.

31.	Netz, R. R., Electrostatics of Counter-Ions at and between Planar Charged Walls: From Poisson-Boltzmann to the Strong-Coupling Theory. *European Physical Journal E* **2001,** *5*, 557-574.

32.	Angelini, T. E.; Liang, H.; Wriggers, W.; Wong, G. C. L., Like-Charge Attraction between Polyelectrolytes Induced by Counterion Charge Density Waves. *Proceedings of the National Academy of Sciences* **2003,** *100*, 8634-8637.

33.	Fauerbach, J. A.; Yushchenko, D. A.; Shahmoradian, S. H.; Chiu, W.; Jovin, T. M.; Jares-Erijman, E. A., Supramolecular Non-Amyloid Intermediates in the Early Stages of Alpha-Synuclein Aggregation. *Biophys. J.* **2012,** *102*, 1127-1136.

34.	Binolfi, A.; Rasia, R. M.; Bertoncini, C. W.; Ceolin, M.; Zweckstetter, M.; Griesinger, C.; Jovin, T. M.; Fernandez, C. O., Interaction of Alpha-Synuclein with Divalent Metal Ions Reveals Key Differences: A Link between Structure, Binding Specificity and Fibrillation Enhancement. *J. Am. Chem. Soc.* **2006,** *128*, 9893-9901.

35.	Nielsen, M. S.; Vorum, H.; Lindersson, E.; Jensen, P. H., Ca2+ Binding to Alpha-Synuclein Regulates Ligand Binding and Oligomerization. *J. Biol. Chem.* **2001,** *276*, 22680-22684.

36.	Wright, J. A.; Brown, D. R., Alpha-Synuclein and Its Role in Metal Binding: Relevance to Parkinson's Disease. *J. Neurosci. Res.* **2008,** *86*, 496-503.

37.	Hoyer, W.; Cherny, D.; Subramaniam, V.; Jovin, T. M., Impact of the Acidic C-Terminal Region Comprising Amino Acids 109-140 on Alpha-Synuclein Aggregation *in Vitro*. *Biochemistry* **2004,** *43*, 16233-16242.

38.	Groenewold, J.; Kegel, W. K., Anomalously Large Equilibrium Clusters of Colloids. *J. Phys. Chem. B* **2001,** *105*, 11702-11709.

39.	Sciortino, F.; Mossa, S.; Zaccarelli, E.; Tartaglia, P., Equilibrium Cluster Phases and Low-Density Arrested Disordered States: The Role of Short-Range Attraction and Long-Range Repulsion. *Phys. Rev. Lett.* **2004,** *93*, 0557011-0557014.

40.   Stradner, A.; Sedgwick, H.; Cardinaux, F.; Poon, W. C. K.; Egelhaaf, S. U.; Schurtenberger, P., Equilibrium Cluster Formation in Concentrated Protein Solutions and Colloids. *Nature* **2004,** *432*, 492-495.

41.   Giasson, B. I.; Murray, I. V. J.; Trojanowski, J. Q.; Lee, V. M. Y., A Hydrophobic Stretch of 12 Amino Acid Residues in the Middle of Alpha-Synuclein Is Essential for Filament Assembly. *J. Biol. Chem.* **2001,** *276*, 2380-2386.

42.   Vilar, M.; Chou, H. T.; Luhrs, T.; Maji, S. K.; Riek-Loher, D.; Verel, R.; Manning, G.; Stahlberg, H.; Riek, R., The Fold of Alpha-Synuclein Fibrils. *Proc. Natl. Acad. Sci. U. S. A.* **2008,** *105*, 8637-8642.

43.   Trexler, A. J.; Rhoades, E., Single Molecule Characterization of Alpha-Synuclein in Aggregation-Prone States. *Biophys. J.* **2010,** *99*, 3048-3055.

44.   Iwai, A.; Masliah, E.; Yoshimoto, M.; Ge, N. F.; Flanagan, L.; Desilva, H. A. R.; Kittel, A.; Saitoh, T., The Precursor Protein of Non-a-Beta Component of Alzheimers-Disease Amyloid Is a Presynaptic Protein of the Central-Nervous-System. *Neuron* **1995,** *14*, 467-475.

45.   Rooijen, B. D. v. Structural and Functional Insights into Interactions of Oligomeric Alpha-Synuclein with Lipid Membranes. PhD Thesis, University of Twente, Enschede, 2009.

FOR TABLE OF CONTENTS ONLY
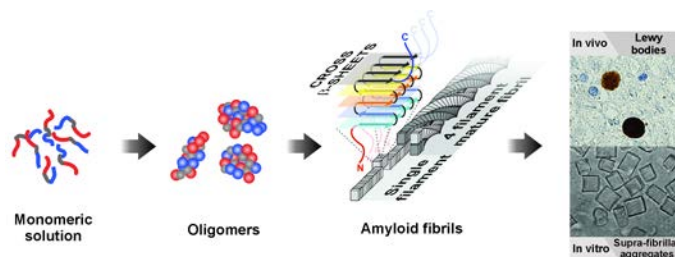
Self-Assembly of Protein Fibrils into Supra-Fibrillar Aggregates: Bridging the Nano- and Mesoscale

Slav A. Semerdzhiev[†], Dirk R. Dekker[†], Vinod Subramaniam[†‡§], and Mireille M.A.E. Claessens[†‡]*

[†] Nanobiophysics, MESA+ Institute for Nanotechnology, Faculty of Science and Technology University of Twente, PO Box 217, 7500 AE Enschede, The Netherlands,

[‡] MIRA Institute for Biomedical Technology and Technical Medicine, University of Twente, PO Box 217, 7500 AE Enschede, The Netherlands

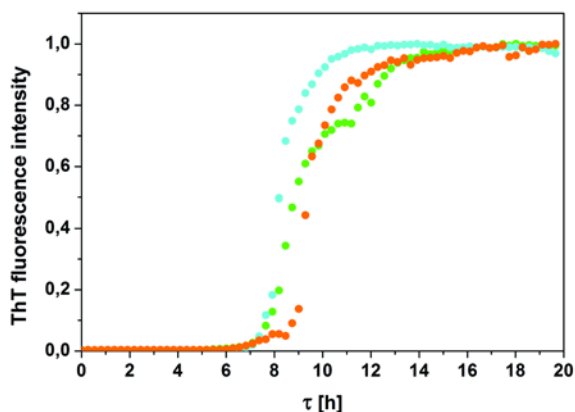[§] FOM Institute AMOLF, Science Park 104, 1098 XG Amsterdam, The Netherlands

Figure S1. Time resolved ThT fluorescence intensity curves obtained during formation of αS supra-fibrillar aggregates (SFAs). The aggregates were formed at 100 μM αS, 2.5 mMCaCl$_2$, 10 mM Tris, pH 7.4 and 37 ^{o}C. The three curves correspond to three separate samples incubated at identical aggregation conditions.
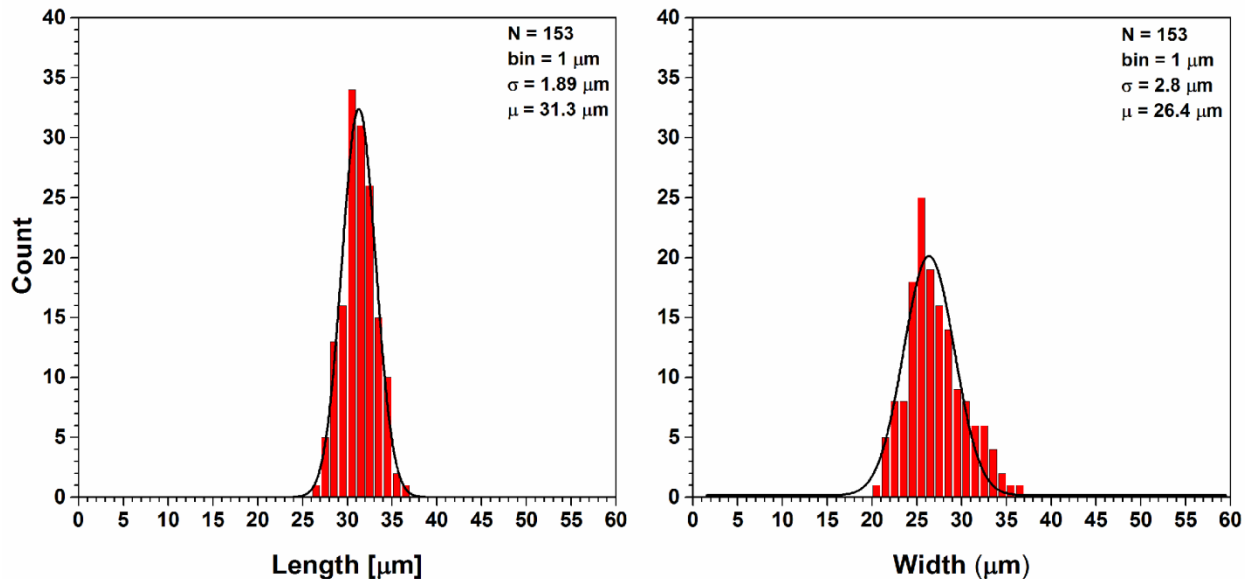

Figure S2. Length and width distribution of the SFAs formed at 100 μM protein concentration, 2 mM CaCl$_2$, 10 mM Tris buffer, pH = 7.4, 37 ^{o}C and in the presence of 5 μM Thioflavin T.
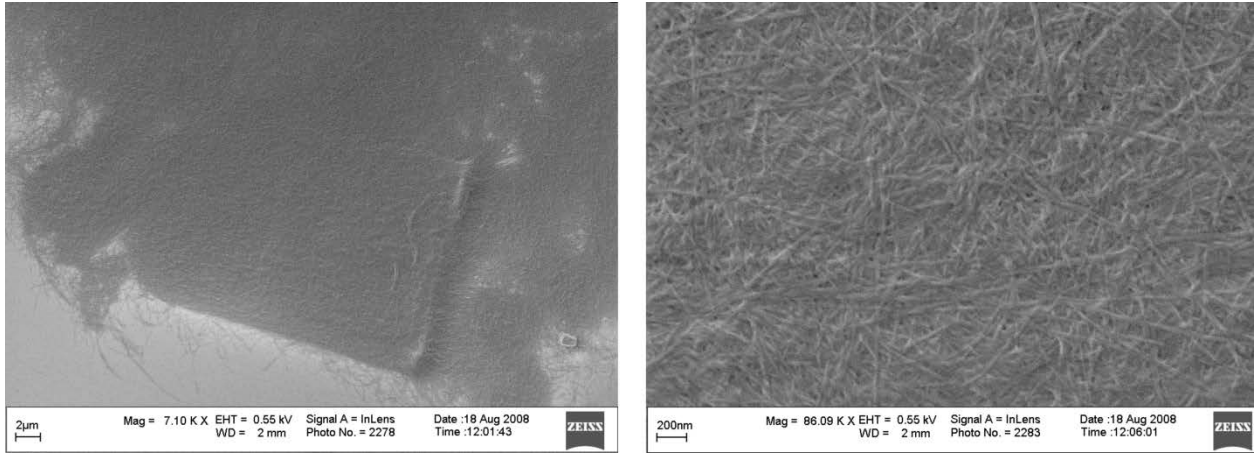
Figure S3. HRSEM micrographs of a supra-fibrillar aggregate. A top view (left) and a zoomed image (right) at the surface of the aggregate.

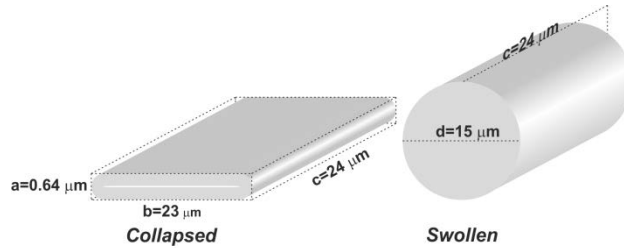**SI 1** Estimation of the water content in the supra-fibrillar aggregates

Figure S4 Geometrical configurations of a swollen and dried supra-fibrillar aggregate used to estimate the water fraction.

In order to estimate the volume of the hydrated and dried aggregate we assume that for both species the circumference P of the cross section remains the same as the aggregate is being dried and collapsed on the mica surface, or:

$$P = \pi d = 2(a + b) \qquad\qquad 1$$

This approximation seems reasonable since there were no cracks or integrity breaches observed (AFM micrographs) at the top layers of the aggregates that would suggest spreading of

the collapsed structures .We also approximate the shape of the collapsed aggregate to a rectangle depicted with dash lines in Figure S4. Using equation1we can calculate back the diameter of the swollen aggregate and subsequently its volume:

$$V_{swollen} = \frac{c\pi d^2}{4} = \frac{c(a+b)^2}{\pi} \approx 4271 \ \mu m^3 \qquad\qquad 2$$

The volume fraction of the water then can be easily estimated:

$$1 - \frac{V_{collapsed}}{V_{swollen}} = 0,92 \qquad\qquad 3$$